

## Search for Axions with the CDMS Experiment

Z. Ahmed,<sup>1</sup> D. S. Akerib,<sup>2</sup> S. Arrenberg,<sup>17</sup> C. N. Bailey,<sup>2</sup> D. Balakishiyeva,<sup>15</sup> L. Baudis,<sup>17</sup> D. A. Bauer,<sup>3</sup> J. Beaty,<sup>16</sup> P. L. Brink,<sup>9</sup> T. Bruch,<sup>17</sup> R. Bunker,<sup>13</sup> B. Cabrera,<sup>9</sup> D. O. Caldwell,<sup>13</sup> J. Cooley,<sup>9</sup> P. Cushman,<sup>16</sup> F. DeJongh,<sup>3</sup> M. R. Dragowsky,<sup>2</sup> L. Duong,<sup>16</sup> E. Figueroa-Feliciano,<sup>5</sup> J. Filippini,<sup>12,1</sup> M. Fritts,<sup>16</sup> S. R. Golwala,<sup>1</sup> D. R. Grant,<sup>2</sup> J. Hall,<sup>3</sup> R. Hennings-Yeomans,<sup>2</sup> S. Hertel,<sup>5</sup> D. Holmgren,<sup>3</sup> L. Hsu,<sup>3</sup> M. E. Huber,<sup>14</sup> O. Kamaev,<sup>16</sup> M. Kiveni,<sup>10</sup> M. Kos,<sup>10</sup> S. W. Leman,<sup>5</sup> R. Mahapatra,<sup>11</sup> V. Mandic,<sup>16</sup> D. Moore,<sup>1</sup> K. A. McCarthy,<sup>5</sup> N. Mirabolfathi,<sup>12</sup> H. Nelson,<sup>13</sup> R. W. Ogburn,<sup>9,1</sup> M. Pyle,<sup>9</sup> X. Qiu,<sup>16</sup> E. Ramberg,<sup>3</sup> W. Rau,<sup>6</sup> A. Reisetter,<sup>7,16</sup> T. Saab,<sup>15</sup> B. Sadoulet,<sup>4,12</sup> J. Sander,<sup>13</sup> R. W. Schnee,<sup>10</sup> D. N. Seitz,<sup>12</sup> B. Serfass,<sup>12</sup> K. M. Sundqvist,<sup>12</sup> M. Tarka,<sup>17</sup> G. Wang,<sup>1</sup> S. Yellin,<sup>9,13</sup> J. Yoo,<sup>3</sup> and B. A. Young<sup>8</sup>

(CDMS Collaboration)

<sup>1</sup>*Department of Physics, California Institute of Technology, Pasadena, California 91125, USA*

<sup>2</sup>*Department of Physics, Case Western Reserve University, Cleveland, Ohio 44106, USA*

<sup>3</sup>*Fermi National Accelerator Laboratory, Batavia, Illinois 60510, USA*

<sup>4</sup>*Lawrence Berkeley National Laboratory, Berkeley, California 94720, USA*

<sup>5</sup>*Department of Physics, Massachusetts Institute of Technology, Cambridge, Massachusetts 02139, USA*

<sup>6</sup>*Department of Physics, Queen's University, Kingston, Ontario, Canada, K7L 3N6*

<sup>7</sup>*Department of Physics, Saint Olaf College, Northfield, Minnesota 55057, USA*

<sup>8</sup>*Department of Physics, Santa Clara University, Santa Clara, California 95053, USA*

<sup>9</sup>*Department of Physics, Stanford University, Stanford, California 94305, USA*

<sup>10</sup>*Department of Physics, Syracuse University, Syracuse, New York 13244, USA*

<sup>11</sup>*Department of Physics, Texas A&M University, College Station, Texas 93106, USA*

<sup>12</sup>*Department of Physics, University of California, Berkeley, California 94720, USA*

<sup>13</sup>*Department of Physics, University of California, Santa Barbara, California 93106, USA*

<sup>14</sup>*Departments of Physics and Electrical Engineering, University of Colorado Denver, Denver, Colorado 80217, USA*

<sup>15</sup>*Department of Physics, University of Florida, Gainesville, Florida 32611, USA*

<sup>16</sup>*School of Physics and Astronomy, University of Minnesota, Minneapolis, Minnesota 55455, USA*

<sup>17</sup>*Physics Institute, University of Zürich, Zürich, Switzerland*

(Received 5 March 2009; published 1 October 2009)

We report on the first axion search results from the Cryogenic Dark Matter Search (CDMS) experiment at the Soudan Underground Laboratory. An energy threshold of 2 keV for electron-recoil events allows a search for possible solar axion conversion into photons or local galactic axion conversion into electrons in the germanium crystal detectors. The solar axion search sets an upper limit on the Primakov coupling  $g_{\text{a}\gamma\gamma}$  of  $2.4 \times 10^{-9} \text{ GeV}^{-1}$  at the 95% confidence level for an axion mass less than  $0.1 \text{ keV}/c^2$ . This limit benefits from the first precise measurement of the absolute crystal plane orientations in this type of experiment. The galactic axion search analysis sets a world-leading experimental upper limit on the axioelectric coupling  $g_{\text{a}\bar{e}e}$  of  $1.4 \times 10^{-12}$  at the 90% confidence level for an axion mass of  $2.5 \text{ keV}/c^2$ .

DOI: 10.1103/PhysRevLett.103.141802

PACS numbers: 14.80.Mz, 29.40.-n, 95.30.Cq, 95.35.+d

The axion has been postulated to solve the strong  $CP$  problem in quantum chromodynamics. The breaking of Peccei-Quinn  $U(1)$  symmetry leaves a pseudo Goldstone boson field [1], interpreted as the axion. Although the original Peccei-Quinn axion model has been ruled out [2,3], “invisible” axion models allow a wide range of axion masses and axion-matter couplings [4]. Astrophysical observations are currently the best strategy to search for these invisible axions [5]. The interior of stars is expected to be a powerful source of axions due to the high abundance of photons and strong electromagnetic fields, which may convert photons into axions. The non-thermal axion production mechanism in the early universe provides a cold dark matter candidate.

Here we report on the first axion search results from the Cryogenic Dark Matter Search (CDMS) experiment. The CDMS Collaboration operates a total of 19 Ge ( $\sim 250$  g each) and 11 Si ( $\sim 100$  g each) crystal detectors at  $\sim 40$  mK in the Soudan Underground Laboratory. The detectors are designed to read out both ionization and phonon signals from recoil events [6]. The ratio of ionization to phonon energy, the ionization yield, enables discrimination of nuclear from electron recoils. The details of the detector structure and operation can be found in Ref. [7]. We report only on germanium detector data from two run periods between October 2006 and July 2007. The analysis follows that detailed in [8], except that we removed timing cuts, which had only been used to discriminate against electron-

recoil events, and included additional detectors whose discrimination against electron-recoil events had been inadequate for the measurement reported in [8], increasing the net exposure to 443.2 kg day before cuts.

The flux of solar axions on Earth can be estimated assuming the standard solar model [9] and a coupling to the  $\mathcal{O}(\text{keV})$  blackbody photons in the core region of the Sun. For axion masses  $\ll 1 \text{ keV}/c^2$ , photon-axion conversion creates a flux of  $\mathcal{O}(\text{keV})$  axions on Earth. The solar axion flux on Earth is given by [10,11]

$$\frac{d\Phi_a}{dE_a} = \frac{6.02 \times 10^{14}}{\text{cm}^2 \text{ s keV}} \left( \frac{g_{a\gamma\gamma} \times 10^8}{\text{GeV}^{-1}} \right)^2 E_a^{2.481} e^{-E_a/1.205}, \quad (1)$$

where  $E_a$  is the energy of the axion in keV and  $g_{a\gamma\gamma}$  is the axion-photon coupling constant.

The axion-photon coupling to the nuclear Coulomb field in the detectors converts axions back into photons of the same energy (Primakov effect). Coherent Bragg diffraction produces a strong correlation between incident beam direction and conversion probability, providing a unique signature of solar axions. The expected event rate can be computed as a function of energy and the orientation of the crystal relative to the location of the Sun [12]. It is given as a function of observed photon energy  $E$  for a given axion momentum transfer  $\vec{q}$  and scattering angle  $\theta$  [13] by

$$\mathcal{R}(E) = 2c \int \frac{d^3q}{q^2} \frac{d\Phi_a}{dE_a} \left[ \frac{g_{a\gamma\gamma}^2}{16\pi^2} |F(\vec{q})|^2 \sin^2(2\theta) \right] \mathcal{W}, \quad (2)$$

where  $\mathcal{W}$  is a detector energy resolution function. The Fourier transform of the electric field in a crystal is given as  $F(\vec{q}) = k^2 \int d^3x \phi(\vec{x}) e^{i\vec{q}\cdot\vec{x}}$ , which depends on  $\phi(\vec{x}) = \sum_i \frac{Ze}{4\pi|\vec{x}-\vec{x}_i|} e^{-(|\vec{x}-\vec{x}_i|)/r} = \sum_G n_G e^{i\vec{G}\cdot\vec{x}}$ , where  $k$  is the photon momentum,  $e$  is the elementary charge,  $\vec{x}_i$  is the position of a germanium atom in the lattice,  $r$  is the screening length of the atomic electric field,  $Z = 32$  for germanium, and  $\vec{G}$  is a reciprocal lattice vector. The structure coefficients  $n_G$  (defined in [13]) account for the face-centered-cubic structure of Ge. The Bragg condition ( $\vec{q} = \vec{G}$ ) can be expressed in terms of the axion energy as  $E_a = \hbar c |\vec{G}|^2 / (2\hat{u} \cdot \vec{G})$ , where  $\hat{u}$  is a unit vector directed towards the Sun.

The expected event rate is calculated based on an accurate measurement of the orientation of each detector with respect to the position of the Sun. We took the specific geometry of the experiment, the live time during data taking, and the seasonal modulation of the solar axion flux due to the changing distance between the Sun and the Earth into account. The geodesic location of the Soudan Underground Laboratory is latitude  $47.815^\circ$  N, longitude  $92.237^\circ$  W, and altitude 210 m below sea level. The geodesic north of the CDMS experimental cavern was measured in 1999 by the Fermilab Alignment Group [14]. A line connecting two survey points along the central axis of the cavern was found to be  $0.165^\circ$  E from true north. By

extension, the main horizontal axis of the CDMS cryostat was found to be  $0.860 \pm 0.018^\circ$  E from true north.

Within the cryostat the 30 CDMS detectors are mounted in five towers of six detectors each. The vertical axis of each tower is aligned with the [001] axis of the detectors. The (110) plane that defines the major flat on each substrate is rotated with respect to its neighbors above and below, such that the detectors form a helix within each tower. The uncertainty in the absolute azimuth orientation of the crystal planes is dominated by an estimated  $3^\circ$  uncertainty in the exact angular position of the tower axes with respect to the central axis of the cryostat. The uncertainty of the zenith angle measurement was estimated to be less than  $1^\circ$ . In Fig. 1 we present the predicted event rate in a germanium detector for an assumed coupling of  $g_{a\gamma\gamma} = 10^{-8} \text{ GeV}^{-1}$ .

In order to sample pure axion interaction candidate events, the software required a single scatter in which one detector had an ionization signal  $>3\sigma$  above the noise, and no other detector had phonon or ionization signals  $>4\sigma$  above mean noise. To make sure the selected events are not due to residual cosmic ray interactions, they are required not to be coincident in time with activity in the veto shield surrounding the apparatus. Candidate events are selected within the  $\pm 2\sigma$  region of the electron-recoil distribution in ionization yield. Data sets taken within 3 d after neutron calibrations are not considered in order to avoid high gamma rates due to activation. The detection efficiency is dominated by the hardware trigger and ionization-threshold software cut at low energy, and by rejection of events with an ionization signal in a detector annular guard electrode, covering 15% of the detector volume. The final energy-dependent exposure after all selection criteria have been applied is the product of the measured efficiency (shown in Fig. 2) and the total expo-

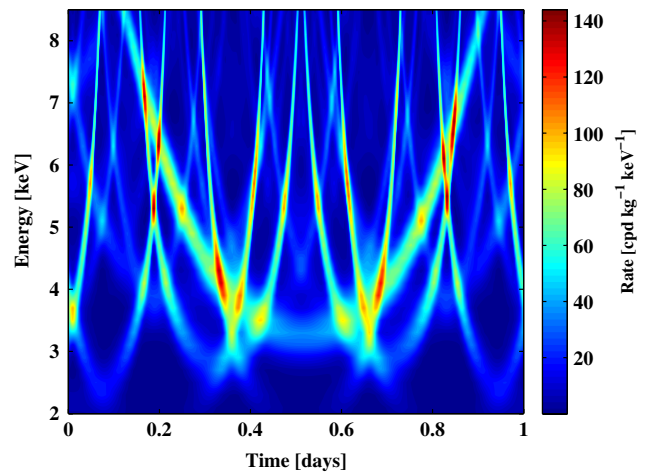


FIG. 1 (color online). Time and energy dependence of the expected solar axion conversion rate in a Ge detector for  $g_{a\gamma\gamma} = 10^{-8} \text{ GeV}^{-1}$ .

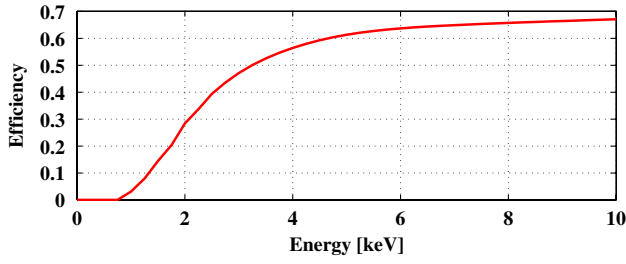


FIG. 2 (color online). Detection efficiency as a function of energy.

sure (443.2 kg day). The average event rate of electron recoil singles below 100 keV in all detectors is stable in time at 16%.

For the germanium detectors considered in this analysis, the summed background rate after correcting for detection efficiency is  $\sim 1.5$  cpd  $\text{kg}^{-1} \text{keV}^{-1}$  (where cpd is counts per day) (Fig. 3). The prominent 10.36 keV line is caused by x rays and Auger electrons from the electron-capture decay of  $^{71}\text{Ge}$ , produced by neutron capture on  $^{70}\text{Ge}$  during  $^{252}\text{Cf}$  calibration of the detectors. The excess in event rate around 6.5 keV (inset) is likely caused by remnant  $^{55}\text{Fe}$  decays from cosmogenic activation. The deexcitation of  $^{55}\text{Mn}$  following the electron-capture decay of  $^{55}\text{Fe}$  yields a total of 6.54 keV of electron-recoil events. We interpolate the energy resolution of the 10.36 keV line (typical  $\sigma/E < 0.04$ ) to the noise level to obtain the energy-dependent resolution of each detector. The analysis window, defined from 2–8.5 keV, is determined by the expected axion flux, background rate, and detection efficiency.

We performed extensive profile likelihood analysis to determine the best fit value of  $g_{a\gamma\gamma}$ . We express the event rate per unit measured energy ( $E$ ), per unit time ( $t$ ), and per detector ( $d$ ) of a solar axion signal with background as

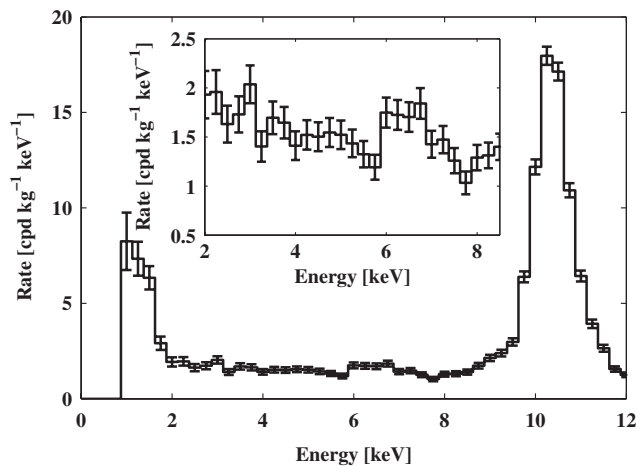


FIG. 3. Coadded, efficiency corrected low energy spectrum of the Ge detectors considered in this analysis. The inset shows an enlargement of the spectrum in the analysis window, taken to be 2–8.5 keV.

$$R(E, t, d) = \varepsilon(E, d)[\lambda \mathcal{R}(E, t, d) + B(E, d)], \quad (3)$$

where  $\varepsilon(E, d)$  is the detection efficiency,  $\mathcal{R}(E, t, d)$  is the expected event rate for a coupling constant  $g_{a\gamma\gamma} = 10^{-8} \text{ GeV}^{-1}$ , and  $\lambda = (g_{a\gamma\gamma} \times 10^8 \text{ GeV})^4$  is the scale factor for the actual value of  $g_{a\gamma\gamma}$ .  $B(E, d)$  is the background described by

$$B(E, d) \equiv C(d) + D(d)E + H(d)/E + \frac{\eta_{6.54}}{\sqrt{2\pi}\sigma_{6.54}} e^{-(E-6.54 \text{ keV})^2/2\sigma_{6.54}^2}, \quad (4)$$

where  $C(d)$ ,  $D(d)$ , and  $H(d)$  are free parameters. The Gaussian term describes a contribution from  $^{55}\text{Fe}$  decays at an energy of 6.54 keV and unknown total rate  $\eta_{6.54}$ . The fitting is done by maximizing the unbinned log likelihood function with respect to  $\lambda$  and the background parameters, for individual events  $i$ :

$$\log(\mathcal{L}) = -R_T + \sum_{i,j} \log[R(E_i, t_i, d_j)], \quad (5)$$

where  $R_T$  is the total sum of the event rate ( $R$ ) over energy, time, and detectors. The scaling factor from the maximization  $\lambda = (1 \pm 1.5) \times 10^{-3}$  is compatible with zero. No indication of solar axion conversion to photons is observed. Given a null observation, we set an upper limit on the coupling constant  $g_{a\gamma\gamma}$ , where the scaling factor  $\lambda$  is obtained by integrating the profile likelihood in the physically allowed region ( $\lambda > 0$ ). The upper limit on the axion-photon coupling,  $g_{a\gamma\gamma} < 2.4 \times 10^{-9} \text{ GeV}^{-1}$  at a 95% C.L. is the only laboratory bound based on the accurate measurement of all crystal orientations of the detectors. None of the previous solar axion search experiments (SOLAX, COSME, DAMA) measured their crystal orientations [15–17], and thus their limits are penalized by picking the least sensitive direction for their solar axion bound. The result of this analysis is compared to other experimental constraints in Fig. 4. Improvement towards the next order of sensitivity requires improvements in both detector exposure and gamma background level. A 100-kg SuperCDMS experiment, with substantially reduced gamma background level ( $\sim 0.1$  cpd  $\text{kg}^{-1} \text{keV}^{-1}$ ) would improve the sensitivity to  $g_{a\gamma\gamma} < 10^{-9} \text{ GeV}^{-1}$ .

In addition to restricting solar axions, the CDMS measurement can be used to limit galactic axions. The DAMA Collaboration interpreted the observed annual modulation signature as a possible detection of axions distributed in the local galactic halo [18,19]. If present, these axions would materialize in our detectors via an axioelectric coupling ( $g_{a\bar{e}e}$ ). However, the nonrelativistic speed of galactic axions causes the conversion rate to be independent of the particle's velocity; thus, the annual modulation of the counting rate is highly suppressed [20], and makes it difficult to fit the DAMA modulation signal into this model. Therefore, the galactic axion model is still an interesting scenario to be explored. Assuming a local ga-

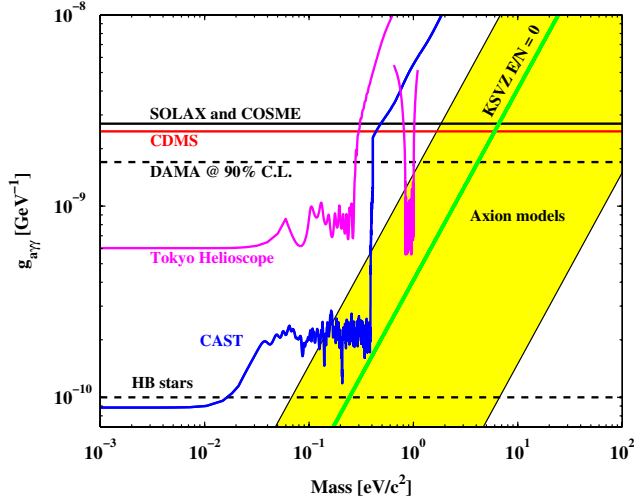


FIG. 4 (color online). Comparison of the 95% C.L. upper limit on  $g_{a\gamma\gamma}$  achieved in this analysis (red solid line) with other crystal search experiments (SOLAX and COSME [15,16] (black solid line) and DAMA (upper black dashed line) [17]) and helioscopes [Tokyo helioscope (magenta solid line) [21] and CAST (blue solid line) [11]]. The indirect constraint of pseudo-scalar from solar neutrino flux bound is also shown [22].

lactic dark matter mass density of  $0.3 \text{ GeV}/c^2/\text{cm}^3$ , the expected event rate [20] is given by

$$R[\text{cpd kg}^{-1}] = 1.2 \times 10^{43} A^{-1} g_{a\bar{a}e}^2 m_a \sigma(pe), \quad (6)$$

where  $m_a$  is the axion mass in  $\text{keV}/c^2$ ,  $A = 73$  for germanium, and  $\sigma(pe)$  is the photoelectric cross section in  $\text{cm}^2$  per atom. We analyzed the energy spectrum using the same electron-recoil data samples used in the solar axion search, as shown in Fig. 3. We performed extensive profile likelihood analysis to search for an excess of event rate above background. The same formalism described in Eqs. (3)–(5) was used, with the term for the expected conversion rate of solar axions  $\mathcal{R}(E, t, d)$  replaced by a Gaussian distribution function representing a spectral line at a given energy or axion mass. We find no statistically significant excess of event rate above background. Lacking a direct constraint on a possible  $^{55}\text{Fe}$  contribution to the spectrum, we set a conservative upper limit, shown in Fig. 5, on the total counting rate in this energy range without any attempt to subtract a possible background contribution. This result excludes significant new galactic axion parameter space in the mass range between  $1.4$  and  $9 \text{ keV}/c^2$ .

In summary, the solar axion search sets an upper limit on the Primakov coupling  $g_{a\gamma\gamma}$  of  $2.4 \times 10^{-9} \text{ GeV}^{-1}$  at the 95% confidence level for an axion mass less than  $\sim 0.1 \text{ keV}/c^2$ . This limit is the first one based on accurate measurements of crystal orientations. The systematic error on the limit is estimated to be 7.9%, which arises from the remaining uncertainty in the alignment of the detector towers' major axes to the central cryogenic axis. The local galactic axion search analysis sets a world-leading experi-

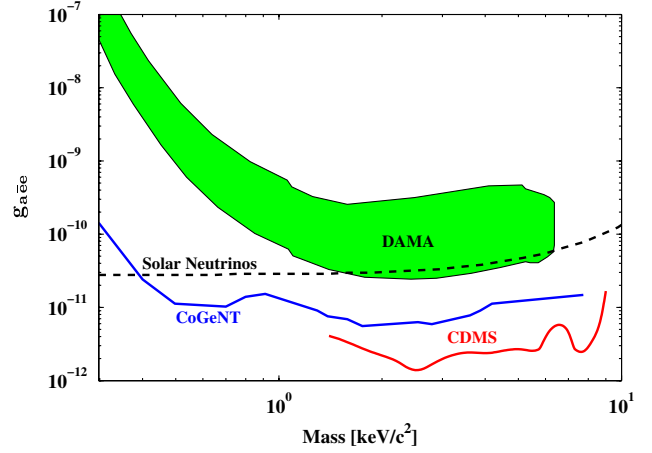


FIG. 5 (color online). The 90% C.L. upper limit on the  $g_{a\bar{a}e}$  coupling constant from this work (red solid line) is shown together with the constraint from CoGeNT experiment (blue solid line) [23]. The indirect constraint of pseudo-scalar from solar neutrino bound (black dashed line) [24] is shown as well. The allowed region of galactic axion interpretation claimed by the DAMA experiment [18] is shown for comparison.

mental upper limit on the axioelectric coupling  $g_{a\bar{a}e}$  of  $1.4 \times 10^{-12}$  at the 90% confidence level for an axion mass of  $2.5 \text{ keV}/c^2$ .

This experiment would not have been possible without the contributions of numerous engineers and technicians; we would like to especially thank Larry Novak, Richard Schmitt, and Astrid Tomada. We thank the CAST and Tokyo helioscope collaborations for providing us with their axion limits. The direction measurement of the true north in the Soudan Underground Laboratory relied on the help from the Fermilab Alignment Group. Special thanks to Virgil Bocean. This work is supported in part by the National Science Foundation (Grants No. AST-9978911, No. PHY-0542066, No. PHY-0503729, No. PHY-0503629, No. PHY-0503641, No. PHY-0504224, and No. PHY-0705052), by the Department of Energy (Contracts No. DE-AC03-76SF00098, No. DE-FG02-91ER40688, No. DE-FG02-92ER40701, No. DE-FG03-90ER40569, and No. DE-FG03-91ER40618), by the Swiss National Foundation (SNF Grant No. 20-118119), and by NSERC Canada (Grant SAPIN 341314-07).

- [1] R.D. Peccei and H.R. Quinn, Phys. Rev. Lett. **38**, 1440 (1977).
- [2] S. Weinberg, Phys. Rev. Lett. **40**, 223 (1978).
- [3] F. Wilczek, Phys. Rev. Lett. **40**, 279 (1978).
- [4] J. E. Kim, Phys. Rev. Lett. **43**, 103 (1979); J. E. Kim, Phys. Rep. **150**, 1 (1987).
- [5] P. Sikivie, Phys. Rev. Lett. **51**, 1415 (1983).
- [6] K.D. Irwin *et al.*, Rev. Sci. Instrum. **66**, 5322 (1995); T. Saab *et al.*, AIP Conf. Proc. **605**, 497 (2002).

- [7] D. S. Akerib *et al.*, Phys. Rev. D **72**, 052009 (2005).
- [8] Z. Ahmed *et al.*, Phys. Rev. Lett. **102**, 011301 (2009).
- [9] J. N. Bahcall and M. H. Pinsonneault, Phys. Rev. Lett. **92**, 121301 (2004).
- [10] S. Andriamonje *et al.*, J. Cosmol. Astropart. Phys. 04 (2007) 010.
- [11] E. Arik *et al.*, J. Cosmol. Astropart. Phys. 02 (2009) 008.
- [12] E. A. Pascos and K. Zioutas, Phys. Lett. B **323**, 367 (1994).
- [13] R. J. Creswick *et al.*, Phys. Lett. B **427**, 235 (1998); S. Cebrian *et al.*, Astropart. Phys. **10**, 397 (1999).
- [14] Fermilab Alignment Group survey at Soudan Underground Laboratory, drawing H5.1, MN1002/3, 1999.
- [15] F. T. Avignone III *et al.*, Phys. Rev. Lett. **81**, 5068 (1998).
- [16] A. Morales *et al.*, Astropart. Phys. **16**, 325 (2002).
- [17] R. Bernabei *et al.*, Phys. Lett. B **515**, 6 (2001).
- [18] R. Bernabei *et al.*, Int. J. Mod. Phys. A **21**, 1445 (2006).
- [19] R. Bernabei *et al.*, Eur. Phys. J. C **56**, 333 (2008).
- [20] M. Pospelov, A. Ritz, and M. Voloshin, Phys. Rev. D **78**, 115012 (2008).
- [21] M. Minowa *et al.*, Phys. Lett. B **668**, 93 (2008).
- [22] G. G. Raffelt, *Stars as Laboratories for Fundamental Physics* (University of Chicago Press, Chicago, 1996).
- [23] C. E. Aalseth *et al.*, Phys. Rev. Lett. **101**, 251301 (2008).
- [24] P. Gondolo and G. G. Raffelt, Phys. Rev. D **79**, 107301 (2009).